

# Role of C/N ratio in a pilot scale Microbial Electrolysis Cell (MEC) for biomethane production and biogas upgrading

Lorenzo Cristiani<sup>\*</sup>, Lorenzo Leobello, Marco Zeppilli, Marianna Villano

Department of Chemistry, Sapienza University of Rome, Piazzale Aldo Moro 5, 00185, Rome, Italy

## ARTICLE INFO

### Keywords:

Biogas upgrading  
Microbial electrolysis cell  
Bioelectromethanogenesis  
Reaction overpotentials

## ABSTRACT

Microbial electrolysis cells (MECs) permit to couple the oxidation of waste organic streams (e.g., wastewater, fermentate or digestate) with the reduction of carbon dioxide into products with a high market value (e.g., methane or acetic acid). MECs exploit the ability of electroactive microorganisms to use a solid electrode as final electron acceptor or donor. Here, a micro pilot tubular MEC has been set up combining the anodic oxidation of the organic matter with the bioelectromethanogenesis reaction in the cathodic chamber. Seven different synthetic feeding solutions, simulating a domestic wastewater or an acidogenic fermentate, have been used to test different C/N ratio on the performance of the MEC bioanode in the range between 25 and 0.4 (molC/molN). As a main result it was found that, under the same operating conditions (i.e., anode potential controlled at + 0.2 V vs SHE and HRT of 0.5 d), a high C/N ratio (e.g., 19 mol/mol) promotes the bioelectrochemical metabolism of the electroactive biofilm. These findings are relevant for a practical application of the technology considering the variable content of carbon and nitrogen in real feedstocks.

## 1. Introduction

The importance of water reclaim is crucial for human footprint reduction, therefore the European union decided to bet on a variety of technologies to intelligently clean water with an energy and material recovery [1]. The anaerobic digestion (AD) is a consolidated technology capable to transform solid or liquid organic waste into biogas and digestate [2]; biogas is a gas mixture mainly composed by carbon dioxide and methane which has a high calorific power and can be converted in electric power by CHP units [3]. Moreover, biogas can be transformed into biomethane, an analogous of natural compressed gas (NCG), through a purification and upgrading step [4,5]. Those steps permit to obtain biomethane through the impurity's removal (such as NH<sub>3</sub>, H<sub>2</sub>S) and increase the CH<sub>4</sub> content up to 95% by the selective removal of the CO<sub>2</sub> [6,7]. The present upgrading technologies, already available at a commercial level are based on physicochemical properties which usually require important capital and operational costs [8]. The increasing market share indicates that the biomethane industry is open for new technologies [9], furthermore, the use of upgraded biogas in transport applications has increased as result of the new opportunities for the use of biogas and benefited from various support schemes and programs [10]. Technological improvements in biogas upgrading

technologies to biomethane could lead to lower energy intensity and improved cost performance that could make biomethane cost competitive with fossil fuel use in transport [11]. The catalytic reduction of CO<sub>2</sub> into CH<sub>4</sub>, also known as Sabatier reaction, has high operational costs, which include Ni based catalysts and high temperature and pressures, however, an interesting and effective approach can be offered using biological methanation of the CO<sub>2</sub> which involve the use of the methanogenesis reaction [12]. During the last years an innovative strategy for biogas upgrading and purification has raised thanks to its ability to abate and reduce CO<sub>2</sub> into CH<sub>4</sub> exploiting the locally produced H<sub>2</sub> [13, 14]. This technology consists in the utilization of a microbial electrolysis cell (MEC) for its ability to reuse wastewater such as digestate or fermentate to extract the reducing power needed to reduce CO<sub>2</sub> into CH<sub>4</sub> [15,16]. This is possible thanks to the ability of some microorganisms called electroactive precisely for their ability to use electrodes as electron donor or acceptor [17–20]. To sum up, if the interacting biofilm uses the solid-state electrode as final electrons acceptor this system can be named bioanode, on the other hand a system consisting in a biofilm using an electrode as electron donor can be named biocathode [21]. Biocathodes are used for many applications such as the bioremediation for polluted waters [22,23] and recovery of nutrients such as phosphates and ammonium [24–27]. The reduction of CO<sub>2</sub> into CH<sub>4</sub> could be

<sup>\*</sup> Corresponding author.

E-mail address: [lorenzo.cristiani@uniroma1.it](mailto:lorenzo.cristiani@uniroma1.it) (L. Cristiani).

<https://doi.org/10.1016/j.renene.2023.04.049>

Received 14 November 2022; Received in revised form 20 March 2023; Accepted 12 April 2023

Available online 15 April 2023

0960-1481/© 2023 The Authors. Published by Elsevier Ltd. This is an open access article under the CC BY license (<http://creativecommons.org/licenses/by/4.0/>).

performed by the biofilm directly taking the reducing power from the electrode (bioelectromethanogenesis [28]) using particular membrane's proteins and/or conductive pili [29] or can be mediated by a molecule able to be reduce/oxidize like  $2\text{H}^+/\text{H}_2$  [30] for hydrogenophilic methanogenesis. To make this possible inside a MEC, an external potential must be applied to obtain the necessary reducing power [31]. Several studies were made to couple a bioanodic oxidation reaction to the cathodic reducing reaction to lower the energetic consumption needed to apply the electric potential [32]. Moreover, a second but more significant  $\text{CO}_2$  removal mechanism, further than its reduction, was studied inside a MEC's cathodic chamber, which exploits the alkalinity generated by the ongoing reactions [28]. Generally, the alkalinity inside the cathodic chamber is generated by the usage of protons, for either hydrogen or methane generation, and for the "non-refueling" of protons caused by the transport of different ionic species through the membrane [33]. Furthermore, many studies suggested to use a MEC to upgrade the biogas outcoming from an anaerobic digester exploiting its double mechanism to remove  $\text{CO}_2$  from a gaseous mixture [32]. Here, a 12L micro-pilot tubular MEC has been built to be integrated with an anaerobic digester in which biogas upgrading is performed inside the cathodic chamber along with the COD oxidation inside the anodic chamber. In a previous study [34], three different nitrogen loading rates (NLR) were tested in the tubular MEC showing a significative change in bioanode performance in terms of electricity production and COD removal. Based on those previous evidence, additional runs at different COD and nitrogen load rate have been conducted in order to study the role of the carbon/nitrogen ratio on the anodic biofilm and in general on the overall tubular MEC's performances, mainly in terms of electricity production, nitrogen recovery, COD removal,  $\text{CO}_2$  abatement,  $\text{CH}_4$  production and energetic consumption. The feasibility of this process showed the great versatility of the MEC which allows to couple target anodic and cathodic processes in one process operated with the use of the sole electrical energy. Moreover, in literature the attempts of scaling up a MEC for biogas upgrading are limited, and this work describes many aspects of the bioelectrochemical upgrading approach to be a starting point for further scale up of the process.

## 2. Materials and method

### 2.1. Set up of the tubular pilot scale MEC

The reactor consisted in a 12 L Plexiglas cylinder, 1.5 m high, divided into two concentric chambers separated by a 2355  $\text{cm}^2$  cation exchange membrane (CEM FKS-PET FUMASEP, Fumatech GmbH 0.013 cm of thickness). The inner/anodic chamber having a volume of 3.14 L, was filled with graphite granules (diameter ranging between 0.2 cm and 4 cm) and inoculated with activated sludge coming from a full-scale municipal wastewater treatment plant located in Treviso (Italy). The outer/cathodic chamber was filled with graphite granules and had a volume of 8.80 L, was inoculated with a different type of inoculum: a digestate coming from an anaerobic digester located in Treviso (Italy). Using a peristaltic pump, the catholyte was continuously recirculated, simultaneously a gaseous mixture containing  $\text{CO}_2$  (30/70  $\text{CO}_2/\text{N}_2$  v/v) was continuously fed from the bottom of the cathodic chamber. The anodic chamber was continuously fed from the bottom with a peristaltic pump at a flow rate of 7 L/d, resulting in a hydraulic retention time (HRT) of 11 h. The feeding solution contained a synthetic mixture of volatile fatty acids (VFA: acetate, propionate and butyrate) to simulate the composition of an acidogenic fermentate. Indeed, as reported in the literature [35] acidogenic fermentate coming from a two-stage AD plant, represents a suitable source of COD to sustain the bioelectrochemical process. VFA were added to a mineral medium (MM) which was composed by:  $\text{NH}_4\text{Cl}$  (0.125 g/L),  $\text{MgCl}_2 \cdot 6\text{H}_2\text{O}$  (0.1 g/L),  $\text{K}_2\text{HPO}_4$  (4 g/L),  $\text{CaCl}_2 \cdot 2\text{H}_2\text{O}$  (0.05 g/L), 10 mL/L of a metal solution, and 1 mL/L of a vitamin solution. Three different concentrations of VFA were used to change the organic loading rate (OLR) from 2.55 gCOD/Ld to 3.82 and

5.11 gCOD/Ld. To increase the nitrogen loading rate (NLR) from 73 mgN/Ld to 2229 mgN/Ld, the  $\text{NH}_4\text{Cl}$  concentration was modified from 0.125 g/L to 3.82 g/L. On the top of the tubular MEC two glass sampling chambers were used to sample both the liquid and the gaseous phase of the anodic and cathodic compartment. A digital barometer was used to measure the pressure of the gaseous inlet to the cathodic chamber. The water electroosmotic diffusion through the CEM increased the liquid level inside the cathodic chamber, therefore a daily spill was performed to maintain constant the liquid volume of the catholyte. The reactor operated at controlled laboratory temperature (25 °C). The MEC was set in a three-electrode configuration with the cathode operated as counter electrode, the anode as working electrode and an Ag/AgCl electrode placed in the anodic chamber as reference electrode. The minimum distance between two graphite granules is the thickness of the membrane (i.e., 0.013 cm) while the maximum distance (between a graphite granule in the middle of the anodic chamber and a granule placed in the external part of the cathodic chamber) is 10 cm. The average distance between two granules placed one inside the anodic and the other in the cathodic chamber at the same height is 5 cm. The anodic potential was controlled by an AMEL 5489 potentiostat at + 0.2 V vs SHE (standard hydrogen electrode) during the whole experimentation. Indeed, due to previous experimentations [32,36], in which many anodic potentials were investigated and evaluated in terms of thermodynamical calculations in order to identify the optimal value for the anodic potential, it was chosen to operate at + 0.2 V vs SHE. The anodic and cathodic potentials were measured using a digital multimeter and an Ag/AgCl reference electrode was placed inside each MEC chamber. Two digital multimeters (Aim-TTI 1604) were connected to the system to continuously measure the flowing current and the potential difference.

### 2.2. Analytical procedures

The chemical oxygen demand (COD) was calculated multiplying the conversion factor (1.067 mgCOD/mg<sub>acetate</sub>; 1.51 mgCOD/mg<sub>propionate</sub>; 1.82 mgCOD/mg<sub>butyrate</sub>) by the VFAs' concentration measured with a gas-chromatograph (GC; DaniMaster, stainless-steel column packed with molecular sieve; He as carrier gas 18 mL/min; oven temperature 175 °C; flame ionization detector (FID) temperature 200 °C). The methane content of the gas phase has been analysed sampling 10  $\mu\text{L}$  of the headspace of the compartments by a gas-tight Hamilton syringe and injecting it into gas-chromatograph (GC; DaniMaster, stainless-steel column packed with molecular sieve; He as carrier gas 18 mL/min; oven temperature 70 °C; flame ionization detector (FID) temperature 200 °C); on the other hand, the  $\text{CO}_2$  and  $\text{H}_2$  determination has been performed by injecting 50  $\mu\text{L}$  of gaseous sample into a DaniMaster gaschromatograph (stainless-steel column packed with molecular sieve;  $\text{N}_2$  as carrier gas 18 mL/min; oven temperature 70 °C; thermal-conductivity detector (TCD) temperature 150 °C). The inorganic carbon was measured by TOC (Total Organic Carbon Analyzer-V CSN; Shimadzu) on filtered samples (0.2  $\mu\text{m}$ ). The Nessler method was used to determine spectrophotometrically (420 nm) the concentration of ammonium ion. The VSS were measured using GF/C filter (47 mm diameter, 1  $\mu\text{m}$  porosity) following the APHA-AWWA-WPCF (1992) procedure.

### 2.3. Theoretical computations

The removed COD is calculated as the difference of the COD inside the feeding solution and the COD in the outlet, as reported by equation (1).

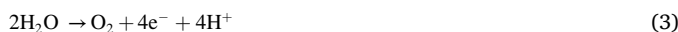
$$\text{COD}_{\text{removed}} = F_{\text{in}} * \text{COD}_{\text{in}} - F_{\text{out}} * \text{COD}_{\text{out}} \quad (1)$$

in which  $\text{COD}_{\text{in}}$  (mg/L) and  $\text{COD}_{\text{out}}$  (mg/L) represent respectively the anodic influent and effluent COD while  $F_{\text{in}}$ (L/d) is the influent and  $F_{\text{out}}$ (L/d) is the effluent flow rate of the anodic chamber (L/d). The

efficiency for COD removal was calculated with equation (2).

$$COD_{removal\ efficiency} = \frac{(COD_{in} - COD_{out})}{COD_{in}} \quad (2)$$

The COD converted into electric current was expressed as electrons' equivalents, considering the water oxidation reaction (equation (3)).



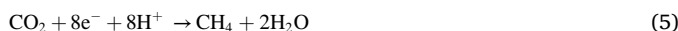
The  $meq_{COD}$  was calculated by using a theoretical conversion factor of 4 meq/32 mgO<sub>2</sub>.

The Coulombic Efficiency (CE%) represents the amount of COD converted into current by its oxidation; it was evaluated as the ratio between the registered electric current and the theoretical electric current producible with the measured COD removal.

$$CE = \frac{meq_i}{meq_{COD}} \quad (4)$$

The cumulative electric charge (meqi) was calculated by integrating the current (A) over time and dividing it by the Faraday's constant (F = 96485 C/eq).

The methane production rate  $rCH_4(mmol)$  (mmol/d) was also expressed in terms of equivalents  $rCH_4(eq)$  (meq/d), considering the theoretical conversion factor of 8 meq/mmolCH<sub>4</sub>, which was computed following the semi-reaction 5.



$$rCH_4(mmol) * 8 = rCH_4(meq) \quad (6)$$

The Cathode Capture Efficiency (CCE, %) is the fraction of the flowing electric current diverted into a reduced product (i.e., methane, acetic acid) inside the cathodic chamber. It was calculated by the ratio between the cumulative equivalents of produced methane ( $meq_{CH_4}$ ) in a fraction of time and the cumulative electric charge flowed in the MEC during the same fraction of time:

$$CCE = \frac{meq_{CH_4}}{meq_i} \quad (7)$$

The following equation was used to calculate the potential loss  $\sum \eta$  (V) which represent the sum of the overpotentials.

$$\sum \eta = \Delta V_{(exp)} - \Delta V_{(meas)} \quad (8)$$

$\Delta V_{exp}$  is the difference of potential measured between the cathode and the anode during the experiment and  $\Delta V_{meas}$  represent the calculated potential difference according to equation (9)

$$\Delta V_{(meas)} = E_{cath(meas)} - E_{an(meas)} \quad (9)$$

In which  $E_{cath(meas)}$  and  $E_{an(meas)}$  are the measured potential vs the reference electrode placed in the respective chamber. The following equation was used to calculate the cathodic potential loss  $\sum \eta_{cat}$  (V) which represent the sum of the cathodic overpotential.

$$\sum \eta_{cat} = E_{cath}^{meas} - E_{cath}^{th} \quad (10)$$

In which  $E_{cath}^{meas}$  is the measured value during the experimental period whereas  $E_{cath}^{th}$  represent the theoretic value calculated with the Nernst equation (11)

$$E_{cath}^{th} = E^0 - \frac{RT}{2F} \ln \frac{pH_2}{[H^+]^2} \quad (11)$$

In which  $E^0$  for  $H^+/H_2$  is equal to 0 V, F is the Faraday's constant (96485 C/mol<sub>e</sub><sup>-</sup>), R is the universal gas constant (8.314 J/molK) and T is the temperature expressed in Kelvin. The  $pH_2$  used is  $10^{-4}$  atm which is the maximum hydrogen's partial pressure on which methanogens work.

The potential losses linked to the pH gradient and to the electrolyte resistance were calculated as reported in Ref. [37].

$$\eta_{pH} = \frac{RT}{F} \ln (10^{(pH_{cathode} - pH_{anode})}) \quad (12)$$

In which, as in equation (11), F is the Faraday's constant (96485 C/mol<sub>e</sub><sup>-</sup>), R is the universal gas constant (8.314 J/molK) and T is the temperature expressed in Kelvin.

$$\eta_{ionic} = I_{ions} \left( \frac{1}{2} R_{anode} + \frac{1}{2} R_{cathode} \right) = I_{ions} \left( \frac{d_{an}}{2A\sigma_{an}} + \frac{d_{cat}}{2A\sigma_{cat}} \right) \quad (13)$$

$I_{ions}$  represent the amount of charges migrated through the membrane (the value is the same of the registered electric current  $\frac{C}{s} = A$ ), R is the resistance of the liquid phase which can be calculated knowing the distance "d" of the electrode from the membrane (cm), the membrane's area "A" (cm<sup>2</sup>) and the conductivity ( $\frac{S}{cm}$ ) of the liquid phase.

#### 2.4. Nitrogen mass balance

The daily nitrogen removal ( $\Delta N$ ; mg/d) has been evaluated by the following equation

$$\Delta N = F_{in} * N_{in} - F_{out} * N_{out} \quad (14)$$

In which  $F_{in}$  and  $F_{out}$  (L/d) are the influent and effluent liquid flow rates, respectively. Moreover,  $N_{in}$  and  $N_{out}$  (mg/L) represent the nitrogen concentration inside the inlet and outlet of the anodic chamber.

Since the nitrogen was in form of ammonium, it could migrate through the CEM, and it was detected inside the cathodic chamber where it was recovered inside the daily spill. A small portion of ammonium is used by microorganisms for growth, it was taken into consideration for the mass balance equation according with the generic biomass composition (C<sub>5</sub>H<sub>7</sub>O<sub>2</sub>N).

$$F_{in} * N_{in} = F_{spill} * \left( VSS_{out\ cat} * 0.12 \frac{g_N}{g_{VSS}} + N_{cat} \right) + F_{out} * \left( N_{out} + VSS_{out\ anode} * 0.12 \frac{g_N}{g_{VSS}} \right) \quad (15)$$

In which  $F_{in}$  and  $F_{out}$  (L/d) are the influent and effluent liquid flow rates, respectively. Moreover,  $N_{in}$  and  $N_{out}$  (mg/L) represent the nitrogen concentration inside the inlet and outlet of the anodic chamber.  $N_{cat}$  represent the nitrogen concentration (mg/L) inside the cathodic chamber and  $F_{spill}$  is the daily spill (L/d) from the cathodic chamber;  $VSS_{out}$  is the measured concentration (mg/L) of the volatile suspended solid (C<sub>5</sub>H<sub>7</sub>O<sub>2</sub>N) inside the anodic or cathodic effluent, 0.12 is the conversion factor used for determining the ammonium nitrogen used for the biomass growth (mgN/mgVSS). Moreover, the nitrogen contribution to the total charge transport inside the MEC has been calculated by using the following equation:

$$i_{ionic} = \frac{[NH_4^+] * F_{spill} * Z * F}{86400s} \quad (16)$$

In which  $F_{spill}$  represent the daily spill (L/d) from the cathodic chamber,  $[NH_4^+]$  is the ammonium concentration (mol/L) inside the cathodic chamber. Z is the amount of charge transported by the cation, F is the Faraday's constant (96485 C/mol<sub>e</sub><sup>-</sup>) and 86400 are the second in one day.

#### 2.5. Inorganic carbon mass balance

The daily removal of CO<sub>2</sub> ( $\Delta CO_2$ , mmol/d) inside the cathodic chamber has been evaluated by equation (17):

$$\Delta CO_2 = Q_{cat,in} * CO_{2\ in} - Q_{cat,out} * CO_{2\ out} \quad (17)$$

in which  $Q_{cat,in}$  (L/d) and  $Q_{cat,out}$  (L/d) are the influent and effluent gas flow rates, respectively. Instead,  $CO_{2,in}$  and  $CO_{2,out}$  (mmol/L) represent

the CO<sub>2</sub> concentrations in the influent and effluent gaseous cathodic streams, respectively.

To make a balance it was considered that the inorganic carbon was present in many forms (i.e., CO<sub>2</sub> and HCO<sub>3</sub><sup>-</sup> ion) inside the system, that the methane production and the CO<sub>2</sub> sorption (as HCO<sub>3</sub><sup>-</sup> ion in the cathodic liquid phases) were the main cathodic CO<sub>2</sub> removal mechanisms. The HCO<sub>3</sub><sup>-</sup> ion in the cathodic chamber is removed by the daily spill.

Equation (18) represents the IC mass balance for the system:

$$\Delta CO_2 = r_{CH_4(\text{mmol})} + VSS_{\text{spilled}} + HCO_3^-_{\text{spilled}} \quad (18)$$

The term  $r_{CH_4(\text{mmol})}$  (mmol/d) represents the production rate of methane while  $VSS_{\text{spilled}}$  and  $HCO_3^-_{\text{spilled}}$  indicate the VSS and bicarbonate daily spilled from the cathodic chamber due to electroosmotic diffusion of water.

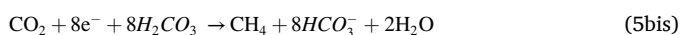
The amount of bicarbonate or VSS spilled is calculated by equations (19) and (19bis)

$$HCO_3^-_{(\text{spilled})} = F_{\text{cat}} * HCO_3^-_{(\text{cat})} \quad (19)$$

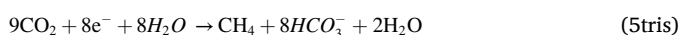
$$VSS_{(\text{spilled})} = F_{\text{cat}} * VSS_{(\text{cat})} * 0.53 \frac{gC}{gVSS} \quad (19\text{bis})$$

Where  $F_{\text{cat}}$  is the amount of liquid spilled daily,  $VSS_{\text{cat}}$  and  $HCO_3^-_{\text{cat}}$  represent the concentration of VSS (C<sub>5</sub>H<sub>7</sub>O<sub>2</sub>N) and bicarbonate inside the cathodic chamber, respectively.

Knowing from equation (5) that for every 8 mol of electrons 8 mol of alkalinity are generated (if there is no migration of protons from the anodic to the cathodic chamber through the CEM, refueling protons inside the cathodic chamber) and 1 mol of CO<sub>2</sub> is reduced into CH<sub>4</sub>, it's possible to calculate a theoretical maximum CO<sub>2</sub> removal capacity of the cathodic chamber. Equation (5) can be rewritten like



Where the 8H<sup>+</sup> are furnished by the carbonic acid, produced from the absorption of CO<sub>2</sub> in water. Therefore, 8 mol of H<sub>2</sub>CO<sub>3</sub> are the result of the absorption of 8 mol of CO<sub>2</sub> which can be added to the one reduced into CH<sub>4</sub>.



Starting from equation 5tris is possible to calculate the amount of CO<sub>2</sub> theoretically removable and express it in many units of measurement.

$$9 \text{ molCO}_{2\text{removed}}^{\text{max}} : 8 \text{ mol}e^- \rightarrow 1.125 \frac{\text{molCO}_{2\text{removed}}^{\text{max}}}{\text{mol}e^-} \rightarrow 1.0074 \frac{\text{molCO}_{2\text{removed}}^{\text{max}}}{Ad} \text{ or } 24.6 \frac{Nd^3 \text{CO}_{2\text{removed}}^{\text{max}}}{Ad} \text{ or } 0.28 \frac{NmLCO_{2\text{removed}}^{\text{max}}}{C} \quad (20)$$

In which  $\text{molCO}_{2\text{removed}}^{\text{max}}$  indicates the maximum number of CO<sub>2</sub> moles removable by a MEC, A is the current flowing (ampere), C is the charge exchanged on the electrode and d are days.

### 3. Results and discussion

#### 3.1. Electric current generation and COD removal

The electric current generated by the anodic biofilm was measured during the whole experimental period. Considering the COD removal all the parameters were determined to evaluate the anodic performance. Theoretically, a higher concentration of substrates should lead to a higher electric current generation, but there are very few data in literature on the effect of a high nitrogen concentration inside the feeding

solution of an electroactive biofilm. For this reason, four C/N ratio were tested, changing it from 0.6 to 0.8; 18.8; 25 (mol/mol) to determine a trend. In order to do this, two OLR values were used: 3.82 and 5.11 gCOD/Ld; for both OLR two NLR (i.e., 73 and 2229 mgN/Ld) were used to compare the results with data of a previous experimentation [34]. During the 3.82 gCOD/Ld experimental periods characterized by a C/N ratio of 0.6 and 18.8 (mol/mol), the electric current generated from the biofilm was  $288 \pm 34$  and  $177 \pm 17$  mA, respectively. The COD removed from the bioanode was  $2.34 \pm 0.7$  gCOD/Ld and  $1.88 \pm 0.68$  gCOD/Ld, respectively, giving a COD removal efficiency of  $75 \pm 8\%$  and  $73 \pm 12\%$ . The corresponding CE were  $17 \pm 0.1\%$  and  $35 \pm 0.3\%$  demonstrating that the bioanode removes more COD with a low C/N ratio without exploiting its potential to produce an electric current probably due a non-electroactive metabolism. It is possible that the limited availability of nitrogen disturbed the metabolism of some other microorganisms with the result of a lower COD consumption. Increasing the OLR to 5.11 gCOD/Ld the electric current decreased to  $133 \pm 15$  and  $191 \pm 14$  mA for a NLR of 2229 and 73 mgN/Ld, respectively. The COD removed was the same i.e.,  $2.7 \pm 1.0$  and  $2.7 \pm 0.7$  gCOD/Ld, suggesting that a high COD concentration boost non-electroactive metabolisms (for example the archaea's metabolism). Also, in this case the CE was higher with a low NLR,  $16 \pm 0.1\%$  against  $11 \pm 0.1\%$ , confirming the trend seen for the other case. Table 1 and Fig. 1 summarize the obtained data showing more clearly the C/N ratio role inside an electroactive bioanode comparing those experimental periods with two published periods in a previous study [34]. During the published periods the OLR was fixed at 2.55 gCOD/Ld and the NLR were 73 and 2229 mgN/Ld, giving a C/N ratio of 12.5 and 0.4 (mol/mol), respectively. The electric currents generated by the bioanode with those conditions were  $190 \pm 14$  and  $157 \pm 7$  mA with a COD removal efficiency of  $29 \pm 11$  and  $89 \pm 20\%$ , respectively. Confirming that a higher NLR leads to a higher COD removal but also to a lower electric current, probably due to a non-electroactive metabolism of some microorganisms which lower the availability of substrates for electroactive microorganisms. This work aims to study how the MEC's performance change by changing two parameters (OLR and NLR) in the feeding solution which simulate possible acidogenic fermentate composition. A possible next step will be using a real matrix coming from a fermenter which is the first stage of a two-stage anaerobic digester. Obviously, the composition of a real fermentate is variable due to the variability of the organic waste loaded inside the fermenter. Therefore, variations of nitrogen and organic carbon concentrations are usual. Moreover, a real matrix has a lower conductivity than the synthetic medium which means a higher resistance of the liquid medium. The resiliency of MECs is fundamental to

work with real wastewaters, and this aspect also need to be further investigated.

#### 3.2. Nitrogen recovery

The CEM permitted the nitrogen recovery in form of ammonium concentrating it inside the cathodic chamber against the concentration gradient. The ammonium nitrogen transport was possible due to the necessity of the system to maintain the electroneutrality inside the chambers during the proceeding of the reactions, indeed, the consumption of protons along with the arrival of electrons leads to migrations of cations from the anodic chamber to the cathodic one through the cation exchange membrane. Changing the OLR (only changing the concentrations of the VFAs, not the mineral medium), the nitrogen

**Table 1**  
Anodic performance of each investigated experimental period (\*previously published periods in Cristiani et al., 2020 [34]).

	2.55 *		3.82		5.11	
	73	2229	73	2229	73	2229
C/N (mol/mol)	12.5	0.4	18.8	0.6	25	0.8
i (mA)	190 ± 14	157 ± 7	288 ± 34	177 ± 17	191 ± 14	133 ± 15
COD removed (gCOD/Ld)	0.63 ± 0.09	1.70 ± 0.2	1.9 ± 0.7	2.3 ± 0.7	2.7 ± 0.7	2.7 ± 1.0
CE (%)	68 ± 14	22 ± 3	35 ± 0.3	17 ± 0.1	16 ± 0.1	11 ± 0.1

removal changes significantly: with an OLR of 3.82 gCOD/Ld it was  $14 \pm 1$  mgN/Ld and  $207 \pm 11$  mgN/Ld with a NLR of 73 mgN/Ld and 2229 mgN/Ld, respectively; with an OLR of 5.11 gCOD/Ld the nitrogen removal was  $5 \pm 1$  and  $138 \pm 10$  mgN/Ld with a NLR of 73 and 2229 mgN/Ld, respectively. The published experimental periods (in Cristiani et al., 2020) i.e., OLR 2.55 gCOD/Ld with a NLR of 73 and 2229 mgN/Ld, permitted a daily removal of  $4 \pm 1$  and  $270 \pm 12$  mgN/Ld. The nitrogen loading rate is 30 times higher than the one used before (73 mgN/Ld), but with an OLR of 2.55 gCOD/Ld the nitrogen removed was 68

times higher than the one obtained with a low NLR. In the other two cases (OLR 3.82 and 5.11 gCOD/Ld) the nitrogen removed was only 15 and 28 times higher, respectively. Thus, those data demonstrate the dependency of the nitrogen removal on more than only one factor: the electric current, which as explained before depends on OLR and the NLR, and the relative amount of nitrogen inside the feeding solution which determines the percentage of ammonium between the total amount of cations present inside the feedstock. Assuming that in a steady state condition the production of microorganisms is equal to the amount of dying microorganisms plus the amount withdrawn with the liquid outlet stream. Knowing that the exiting VSS were steadily  $417 \pm 16$  mg/d during every experimental period, we can assume that  $50 \pm 2$  mgN/d are exiting from the system as microorganism (assuming a molecular formula of  $C_5H_7O_2N$ ). Knowing from the VSS analysis, that changing the C/N ratio did not change significantly the amount of microorganisms inside the system we can exclude microbial growth as main nitrogen removal mechanisms. Therefore, the two main factors influencing the nitrogen recovery and removal are the electric current and the percentage of ammonium between the total amount of cations inside the feedstock. Fig. 2 clearly shows that in this system the best C/N ratio, in terms of percentage of nitrogen recovery inside the liquid outlet from the cathodic chamber, was 18.8 molC/molN i.e., OLR of 3.82

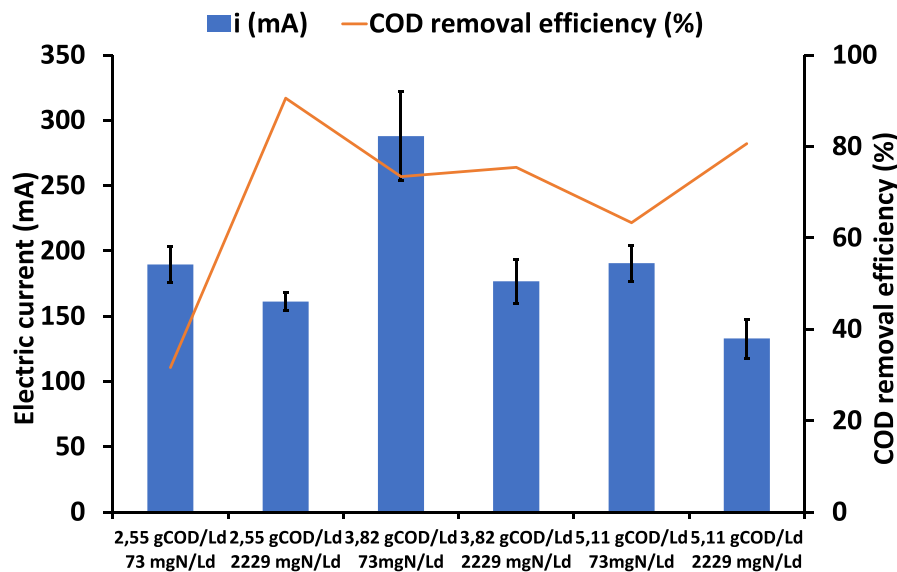


**Fig. 1.** Anodic performance registered during the experimental periods (both periods characterized by an OLR of 2.55 gCOD/Ld were published in Cristiani et al., 2020 [34]).

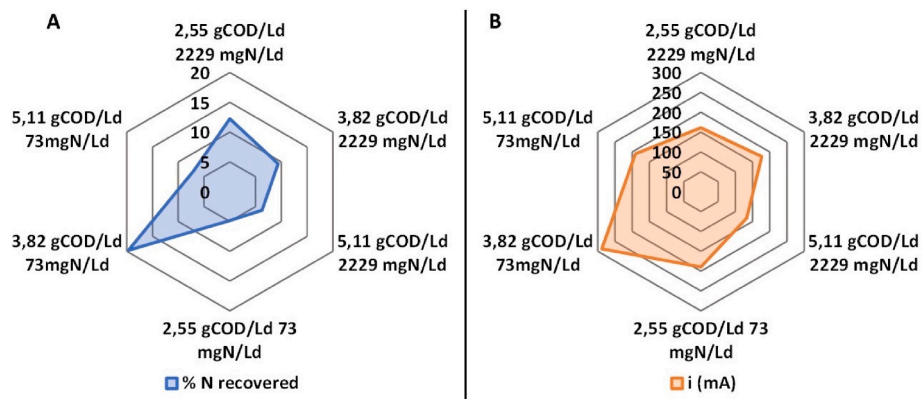


**Fig. 2.** Nitrogen's recovering efficiencies (A) and electric current obtained during the different C/N ratios (B) (both periods characterized by an OLR 2.55 gCOD/Ld were published in Cristiani et al., 2020 [34]).

gCOD/Ld and NLR of 73 mgN/Ld. This feeding solution permitted to obtain the highest electric current but at the same time had the lowest percentage of ammonium with respect of all the present cations (like all the experimental periods characterized by a NLR of 73 mgN/Ld, i.e., 4.7% molN/mol<sub>cations</sub> or 4.6% CNH<sub>4</sub><sup>+</sup>/C<sub>cations</sub>).

The migration of ammonium, along with the other cations, transports charges and therefore permitted to maintain the electroneutrality inside the system. The quantity of migrated ammonium depends on the composition of the feeding solution and on the amount of electric current, for this reason the differences between the results obtained with two NLR were net. Potassium was the most present cation inside the feeding solution 92.3% (molK<sup>+</sup>/mol<sub>cations</sub> or 89.6% Charges/C<sub>cations</sub>) during the 73 mgN/Ld periods and 69.5% (molK<sup>+</sup>/mol<sub>cations</sub> or 67.9% Charges/C<sub>cations</sub>) during the 2229 mgN/Ld periods. For this reason, it is probable that most of the charge was transported through the membrane by this cation. Knowing that the ions' radiuses (which are 147 p.m. and 138 p.m. for NH<sub>4</sub><sup>+</sup> and K<sup>+</sup>, respectively) are similar, the interesting result consist in the amount of migrated ammonium: the feeding solution used during the 2229mgN/Ld periods was characterized by a percentage of ammonium, with respect of the cations' sum, of 28.2% (molN/mol<sub>cations</sub> or 27.6% CNH<sub>4</sub><sup>+</sup>/C<sub>cations</sub>), but the amount of charge counterbalanced by the ammonium's migration was 119 ± 1, 83 ± 1 and 74 ± 4% with an OLR of 2.55, 3.82 and 5.11 gCOD/Ld, respectively. To summarize, as shown in Table 2, the micropilot reactor permitted an efficient nitrogen removal by concentrating it inside the catholyte and the increase of the ammonium concentration inside the feeding solution enhanced this performance even more than expected. In order to recover nitrogen, it is possible to add to the daily spilled solution (which has a high ammonium concentration) phosphate and magnesium (mole-to-mole ratio 1:1:1) which will give a struvite precipitation (MgNH<sub>4</sub>PO<sub>4</sub>·6H<sub>2</sub>O). The struvite has a low solubility in water therefore it is widely utilized for phosphate or nitrogen recovery from wastewaters.

### 3.3. Methane production

The cathodic chamber was inoculated with digestate, which contains methanogens capable of exploiting the reducing power furnished by the system to transform CO<sub>2</sub> into CH<sub>4</sub>. A gaseous mixture containing 30% CO<sub>2</sub> (v/v) was continuously fed inside the cathodic chamber to perform the upgrading of a synthetic biogas (for security reasons the 70% (v/v) left was not CH<sub>4</sub> but N<sub>2</sub>, equally inert and with a similar henry's constant). During the experimental periods characterized by a NLR of 2229 mgN/Ld, as a results of the nitrogen migration, the concentration of ammonium in the catholyte resulted over 1.4 gN/L. This high concentration has partially inhibited the methane production which reached its maximum (10 ± 1 mmol/d) during the period characterized by an OLR of 3.82 gCOD/Ld (during the period characterized by an OLR of 5.11 gCOD/Ld the CH<sub>4</sub> production was 6 ± 1 mmol/d). As a result, the CCE were 51 ± 4% and 42 ± 5% for the OLR 3.82 and 5.11 gCOD/Ld periods, respectively. In contrast, the methane production during the experimental periods characterized by a NLR of 73 mgN/Ld was 18 ± 1 and 23 ± 4 mmol/d with an OLR of 3.82 and 5.11 gCOD/Ld, respectively. The

**Table 2**  
Nitrogen concentration and removal during the six experimental periods (\* published periods in Cristiani et al., 2020 [34]).

OLR (gCOD/Ld)	2.55*		3.82		5.11	
NLR (mgN/Ld)	73	2229	73	2229	73	2229
i (mA)	190 ± 14	157 ± 7	288 ± 34	177 ± 17	191 ± 14	133 ± 15
[NH <sub>4</sub> <sup>+</sup> ] <sub>cathode</sub> (mgN/L)	101 ± 9	1985 ± 78	95 ± 11	2244 ± 104	89 ± 13	1460 ± 91
Nitrogen removal (mg/Ld)	4 ± 1	270 ± 12	14 ± 1	207 ± 11	5 ± 1	138 ± 10
mA transported by NH <sub>4</sub> <sup>+</sup> (%)	1 ± 1	119 ± 1	4 ± 1	83 ± 1	2 ± 1	74 ± 4

resulting CCE were 61 ± 1 and 108 ± 11%, confirming that a low NH<sub>4</sub><sup>+</sup> concentration it's preferable inside the catholyte. Therefore, as shown in Fig. 3, for an efficient production of methane is preferable to start from feedstock with a low concentration of ammonium. Or as a solution, is important to remove the ammonium from the catholyte to limit the inhibition of the methanogens. To compare with the published periods, with an OLR of 2.55 gCOD/Ld the methane production inside the cathodic chamber was 9 ± 1 and 10 ± 1 mmol/d with a NLR of 73 and 2229 mgN/Ld, respectively. The resulting CCE was 42 ± 3 with a NLR of 73 mgN/Ld (which is the lowest CCE obtained with a low NLR) and 54 ± 4% with a NLR of 2229 mgN/Ld (which is the highest CCE obtained with a high NLR).

### 3.4. CO<sub>2</sub> abatement

CO<sub>2</sub> removal in the cathodic chamber of the tubular MEC was assessed by setting the corresponding mass balance which consider the CO<sub>2</sub> reduction into methane and the CO<sub>2</sub> transformation into HCO<sub>3</sub><sup>-</sup> for the alkalinity generated in the cathodic chamber. CO<sub>2</sub> sorption was driven by the continuous alkalinity production generated by the migration of cationic species like ammonium instead of protons. The alkalinity generation is directly correlated to the average electric current flowing in the circuit; thus, a higher current density should promote a higher CO<sub>2</sub> sorption. The bicarbonate produced inside the cathodic chamber does not migrate or diffuse through the CEM, thereby, in a steady state condition, the produced HCO<sub>3</sub><sup>-</sup> is easily calculated measuring the amount of inorganic carbon (IC) daily spilled from the cathodic chamber. Predictably, the highest CO<sub>2</sub> removal was obtained concurrently with the highest obtained electric current, i.e., 264 ± 11 mmol/d and 288 ± 34 mA, respectively.

Table 3 describes the results registered during each experimental period. The CO<sub>2</sub> removal spilling the catholyte from the cathodic chamber contributed for more than the 90%, confirming that the generation of alkalinity is the main abatement mechanism. The CO<sub>2</sub> reduction to methane contributed quite less (from 3 to 14%), for example, during the period characterize by an OLR 5.11 gCOD/Ld and a NLR 73 mgN/Ld the methane production contributed only for the abatement of 14 ± 1% of the total CO<sub>2</sub> removed; moreover, the absorption of CO<sub>2</sub> with the production of HCO<sub>3</sub><sup>-</sup> contributed for the 84 ± 1%. The remaining 2% of the CO<sub>2</sub> removed consist in VSS and precipitation of MgCO<sub>3</sub> and CaCO<sub>3</sub>. The CO<sub>2</sub> sorption favored by the generated alkalinity remains the main removal mechanism. For every mole of produced CH<sub>4</sub>, 8 H<sup>+</sup> (4 to produce 2 H<sub>2</sub>O and 4 for the CH<sub>4</sub>) are consumed, therefore 8 mol of alkalinity are generated. With the generated alkalinity is possible to remove 8 mol of CO<sub>2</sub> producing 8 mol of HCO<sub>3</sub><sup>-</sup>, subsequently, the theoretical amount of CO<sub>2</sub> removable through methanogenesis is only 1/9 (8 through alkaline water sorption plus 1 through methanogenesis; 1/9 ≅ 11%) of the removed CO<sub>2</sub>. The CO<sub>2</sub> removal did change significantly, probably due to differences between the cathodic current densities (knowing that the cathodic chamber's volume is 8.8 L, the current densities result between 18 ± 1 and 33 ± 4 A/m<sup>3</sup>). Interestingly, the amount of CO<sub>2</sub> daily removed divided by the current density gives a value which describes if the system is over or underperforming. Knowing from equations (5) and (20) that, theoretically, a maximum of 9/8 mol of CO<sub>2</sub> are abated for every mole of electrons flowing in the cathodic chamber, this value is 1.125 molCO<sub>2 removed</sub><sup>max</sup>/mol e<sup>-</sup> or 24.6 Ndm<sup>3</sup>CO<sub>2 removed</sub><sup>max</sup>. In Table 3 are reported those values for each experimental period, showing that in only two cases (NLR of 73 mgN/Ld and OLR of 3.82 and 5.11 gCOD/Ld) the MEC has underperformed with a resulting value of 1.0 ± 0.1 molCO<sub>2 removed</sub><sup>max</sup> for both cases. This means that during every other experimental period, the MEC has abated more CO<sub>2</sub> than the one theoretically predictable. Reading Table 3, is easily noticeable that a low NLR affects negatively the CO<sub>2</sub> abatement. The performance value is always higher with a high NLR, and in case of a OLR of 5.11 gCOD/Ld the result is even 1.7 ± 0.1

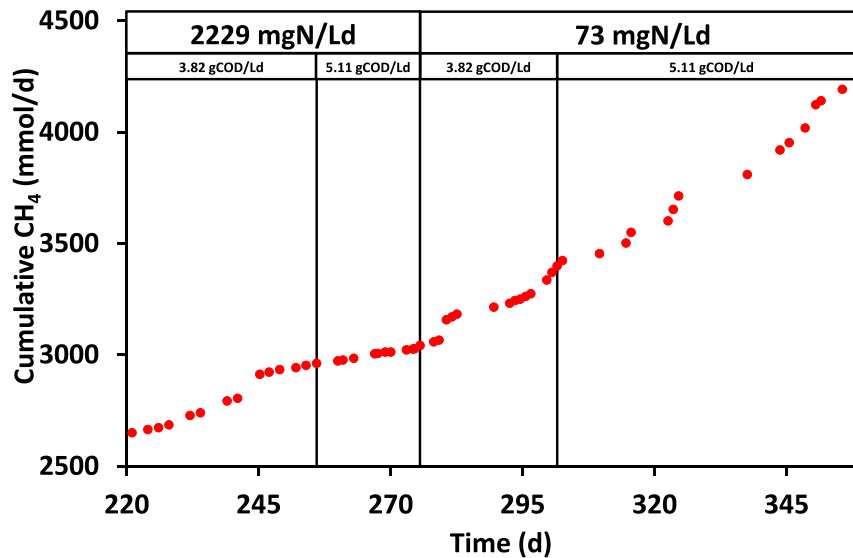


Fig. 3. Methane production inside the system during the four experimental periods.

Table 3

Inorganic carbon mass balance during the experimental periods (\* published periods in Cristiani et al., 2020 [34]).

OLR (gCOD/Ld)	2.55*		3.82		5.11	
	73	2229	73	2229	73	2229
i (mA)	190 ± 14	157 ± 7	288 ± 34	177 ± 17	191 ± 14	133 ± 15
CO <sub>2</sub> removal (mmol/d)	243 ± 15	223 ± 11	264 ± 11	228 ± 15	163 ± 12	202 ± 13
HCO <sub>3</sub> <sup>-</sup> spilled (mmol/d)	55 ± 5	195 ± 20	248 ± 10	215 ± 7	138 ± 10	193 ± 15
CH <sub>4</sub> production (mmol/d)	9 ± 1	10 ± 1	18 ± 1	10 ± 1	23 ± 4	6 ± 1
Conversion yield CO <sub>2</sub> → CH <sub>4</sub> (%)	4 ± 1	4 ± 1	7 ± 1	4 ± 1	14 ± 3	3 ± 1
$\frac{molCO_2\ removed}{mole^-}$	1.4 ± 0.1	1.6 ± 0.1	1.0 ± 0.1	1.4 ± 0.1	1.0 ± 0.1	1.7 ± 0.1

$\frac{molCO_2}{mole^-}$ , suggesting that the feeding solution's concentration has an impact on the CO<sub>2</sub> abatement. Future studies will try to understand how the NLR or more generally the feeding solution's composition affects the CO<sub>2</sub> abatement. The latter could be enhanced by the interaction of different cations inside the catholyte or for a similar conductivity of the two liquid phases.

### 3.5. Characterization of the MEC's potential loss

During the whole experimental period the electrodes' potentials were monitored and measured to obtain a more complete picture of the MEC performance. It is important to take into account that the pH of both the anode feeding solution and the anolyte solution did not change significantly; their value resulted on average  $6.8 \pm 0.1$  and  $6.7 \pm 0.2$ , respectively. The anodic potential was controlled by a potentiostat with a three-electrode configuration at + 0.2 V vs SHE, therefore, the cathodic potential was the one able to change significantly. With higher electric current flowing inside the MEC, the potential difference increased, and along with this increase the potential loss has raised. During the experimental period characterized by an OLR of 3.82 gCOD/Ld and a NLR of 73 mgN/Ld the electric current was  $288 \pm 34$  mA, the  $\Delta V$  was  $-3.3 \pm 0.2$  V and the potential loss was  $2.1 \pm 0.2$  V, in contrast, during the experimental period characterized by an OLR of 5.11 gCOD/Ld and by a NLR 2229 mgN/Ld the electric current was  $133 \pm 15$ , the potential difference was  $-1.2 \pm 0.1$  and the potential loss was  $0.5 \pm 0.1$  V.

The potential drop could be explained by the conductivity of the anolyte which changed by varying the C/N ratio inside the feeding solution. A higher concentration of ammonium implies a higher conductivity and a lower difference with the conductivity of the catholyte. Simultaneously a higher concentration of ammonium inside the anolyte lowers the osmotic pressure. Moreover, a higher concentration of ammonium increases the availability of cations capable of migration through the CEM lowering the potential loss for the migration of cations. Therefore, the ionic loss was calculated following equation (13) reported in Ref. [37]. Ionic losses are significant higher for a system with low conductive liquid phases and as predicted, are significant higher for a low NLR. Along with the ionic losses, the pH split losses were calculated following equation (12) and considering the differences between the pHs of the catholyte and the anolyte. The anolyte's and catholyte's pHs were stable during each experimental periods and there were small differences between the two values (on average  $6.7 \pm 0.2$  vs.  $6.6 \pm 0.3$ ), therefore pH gradient losses were similar during every experimental period. The total potential loss is significantly higher than the sum of the

Table 4

Summary of the potential losses during the experimental periods (\* published periods in Cristiani et al., 2020 [34]).

OLR (gCOD/Ld)	2.55*		3.82		5.11	
	73	2229	73	2229	73	2229
i (mA)	190 ± 14	157 ± 7	288 ± 34	177 ± 17	191 ± 14	133 ± 15
$\Delta V$ (V)	-2.6 ± 0.2	-1.4 ± 0.1	-3.3 ± 0.2	-1.6 ± 0.1	-2.0 ± 0.1	-1.2 ± 0.1
E <sub>cat</sub> (V vs SHE)	-1.0 ± 0.1	-0.6 ± 0.1	-1.0 ± 0.1	-0.9 ± 0.1	-1.2 ± 0.1	-0.5 ± 0.1
$\eta_{leath}$ (V)	0.7 ± 0.1	0.3 ± 0.1	0.7 ± 0.1	0.6 ± 0.1	0.9 ± 0.1	0.2 ± 0.1
$\eta_{pH}$ (V)	0.08 ± 0.01	0.02 ± 0.01	0.04 ± 0.01	0.05 ± 0.01	0.05 ± 0.01	0.06 ± 0.01
$\eta_{ionic}$ (V)	0.10 ± 0.01	0.04 ± 0.01	0.16 ± 0.01	0.04 ± 0.01	0.10 ± 0.01	0.04 ± 0.01
$\sum \eta$ (V)	1.3 ± 0.1	0.5 ± 0.1	2.1 ± 0.2	0.5 ± 0.1	0.6 ± 0.1	0.5 ± 0.1

ionic and pH gradient losses, this indicates that the main losses should be the ohmic drop losses. This result is inevitable inside big electrochemical systems, such as the one used for those experiment. Moreover, the cathodic overpotential was calculated following equations (10) and (11). Since the cathodic pH were stable and the  $pH_2$  was considerate stable too (at  $10^{-4}$  atm), the theoretic cathodic potential was more or less  $-0.33 \pm 0.02$  V vs SHE for each condition. Subsequently, the cathodic potential losses variate along with the variation of the measured cathodic potential (see Table 4). The cathodic losses raised along with the electric current, suggesting an ohmic resistance or/and a charge transfer resistance. Also, this result is inevitable while using high scale electrochemical systems. Using materials with better performances than graphite granules could represent a solution, but the investment cost will inevitably raise. A possible comparison can be made with a twin system described in Cristiani et al., 2021 [32]. The electrodic material used was the same (i.e., graphite granules), the microorganisms inoculated were coming from the same bioreactors (Treviso), the only different was the membrane which was an AEM (anionic exchange membrane) instead of a CEM. The anodic potential was controlled at  $+0.2$  V vs SHE and during the first period described in Cristiani et al., 2021 [32] the OLR was raised from 2.55 to 3.82 and to 5.11 gCOD/Ld (NLR 73 mgN/Ld). The calculated cathodic overpotential ( $\eta_{\text{cath}}$ ) were 0.99, 1, 2.18 V, respectively. Those overpotentials are significantly higher than the ones obtained with the system described in this work (i.e., BES equipped with a CEM), which are in between  $0.2 \pm 0.1$  V and  $0.9 \pm 0.1$  V. The enhancement of the performance could be explained by the higher bicarbonate concentration inside the catholyte ( $13 \pm 1$  g/L vs  $2 \pm 1$  g/L) due to its catalytic effect [38]. The CEM membrane does not permit the diffusion of bicarbonate produced by the absorption of  $\text{CO}_2$ . The graphite granules were used as electrodic material for their compatibility with biofilms formation, as well as for their good electrochemical properties such as conductivity and low degradability at the used potentials and, more importantly, for their low cost. A material with better performance will probably cost more, and for a pilot scale electrochemical system, in which the necessary electrodic material is a significant amount, will lead to a significant increase of the necessary starting budget.

### 3.6. Energetic evaluation

For every period the energetic consumptions were evaluated for each process i.e.,  $\text{CO}_2$  abatement, COD removal and nitrogen recovery. Table 5 shows every performance for each experimental period, it is notable that an increase of the entering COD decreases the energetic consumption necessary to abate COD. As previously demonstrated, lowering the C/N ratio increases the COD abatement and decreases the overpotentials, moreover a high OLR increases the COD removal. The

**Table 5**

Energetic performance of the system during the experimental periods (\* published periods in Cristiani et al., 2020 [34]).

OLR (gCOD/Ld)	2.55*		3.82		5.11	
	73	2229	73	2229	73	2229
NLR (mgN/Ld)						
C/N (mol/mol)	12.5	0.4	18.8	0.6	25	0.8
i (mA)	190 ± 14	157 ± 7	288 ± 34	177 ± 17	191 ± 14	133 ± 15
ΔV (V)	-2.6 ± 0.2	-1.4 ± 0.1	-3.3 ± 0.2	-1.6 ± 0.1	-2.0 ± 0.1	-1.2 ± 0.1
kWh/kgN	388 ± 21	2 ± 1	196 ± 14	4 ± 1	201 ± 17	3 ± 1
kWh/Nm <sup>3</sup>	1.2 ± 0.1	0.8 ± 0.1	8.3 ± 0.5	1.5 ± 0.4	2.6 ± 0.1	0.8 ± 0.1
CO <sub>2</sub>	6.1 ± 0.4	1.0 ± 0.1	4.2 ± 0.1	0.9 ± 0.1	1.1 ± 0.1	0.5 ± 0.1
kWh/kgCOD	0.4	0.1	0.1	0.1	0.1	

combination of those three factors explains the very good performance registered during the last experimental period, which was characterized by an OLR of 5.11 gCOD/Ld and a NLR of 2229 mgN/Ld (i.e., 0.5 kWh/kgCOD). This energetic consumption is lower than 1.1 kWh/kgCOD reported in literature for wastewater treatment (Mancini et al., 2021). Generally, COD is removed efficiently, with a low consumption of energy, during every experimental period with a NLR of 2229 mgN/Ld for the high COD removal obtained with a low C/N ratio. The  $\text{CO}_2$  abatement does not change significantly during every experimental period probably because, even if the C/N affects the bioanodic performance which is linked to the cathodic one, the current density does not change significantly due the high volume of the cathode (i.e., 8.8 L). What does change during the experiment are the overpotentials. With a high NLR the conductivity of the feeding solutions was significantly higher, giving a low difference between the anolyte's and catholyte's conductivity. Thus, the average energy spent for a normal cubic meter of  $\text{CO}_2$  abated changes while changing the C/N ratio: with the highest C/N ratios (18.8 and 25 mol/mol) 8.3 or 2.6 kWh were necessary to abate 1 Nm<sup>3</sup> of  $\text{CO}_2$ , on contrary, with a C/N ratio of 0.4 or 0.8 mol/mol was necessary only 0.8 kWh to abate 1 Nm<sup>3</sup> of  $\text{CO}_2$ . At last, the energy spent to recover 1 kg of nitrogen does change significantly changing the composition of the feeding solution: working with a low NLR produces a high consumption to recover 1 kg of nitrogen; the best performance obtained with a NLR of 73 mgN/Ld was  $196 \pm 14$  kWh/kgN; contrarily, having a high NLR permits to recover 1 kg of nitrogen spending only 2 kWh (for a C/N of 0.4 mol/mol). Furthermore, this experiment demonstrates the high versatility of the bioelectrochemical systems, which are capable of treating wastewaters without losing the effectiveness even if its content of organic substrates and its nitrogen concentration change significantly. Moreover, is fundamental to remember that this system does three different processes at once with only one energetic consumption. Table 5 summarizes the energetic consumption for the single process performed by the system.

### 4. Conclusions

The herein studied MEC confirmed to be an appealing system to exploit the residual reducing power inside a synthetic fermentate, to recover nitrogen inside the latter, and to simultaneously abate  $\text{CO}_2$  inside a biogas. The study on the C/N ratio is fundamental due to the extreme heterogeneity of the wastewaters, which are the feeding solution of this type of MEC. The anodic performances do change significantly changing this parameter: with a high NLR the COD abatement is higher than the one obtained with a low NLR, but it activates a non-electroactive metabolism, therefore the CE decreases. Enhancing the OLR does enhance the electric current production with an upper limit between 3.82 gCOD/Ld and 5.11 gCOD/Ld probably due to a microorganisms' inhibition for the high concentration of substrates. Therefore, to obtain high electric current is preferable to maintain low the NLR (i.e., 73 mgN/Ld) and a medium OLR (i.e., 3.82 gCOD/Ld). The recovery of nitrogen works better with a high electric current which promotes the migration of ammonium through the CEM. For this reason, the best configuration, in terms of percentage of nitrogen recovered, was the one with a high electric current:  $288 \pm 34$  mA, obtained with an OLR of 3.82 gCOD/Ld and a NLR of 73 mgN/Ld. In terms of most nitrogen daily recovered with the lowest energetic consumption, the best OLR was 2.55 gCOD/Ld with a NLR of 2229 mgN/Ld, which permitted to recover  $270 \pm 12$  mgN/Ld. The high concentration of ammonium inside the cathodic chamber partially inhibited the methanogenesis, for this reason the best  $r\text{CH}_4$  was registered with a NLR of 73 mgN/Ld ( $23 \pm 4$  mmol/d, obtained setting the OLR at 5.11 gCOD/Ld). The low NLR permitted a high COD conversion into electric current which generates alkalinity inside the cathodic chamber, the latter boosted the  $\text{CO}_2$  abatement, therefore the best OLR and NLR were 3.82 gCOD/Ld and 73 mgN/Ld, respectively. The high NLR permitted to obtain lower overpotential either for the high conductivity of the anolyte, comparable to



the one measured inside the catholyte, or for the lower electric current generated from the bioanode. Moreover, the energetic consumptions calculated for each process demonstrate how a low C/N ratio permits to abate CO<sub>2</sub>, remove COD and recover nitrogen with the lowest consumption. To sum up, the experimental period characterized by a NLR of 2229mgN/Ld and by an OLR of 5.11 gCOD/Ld permitted to obtain a good CO<sub>2</sub> and COD removal, the lowest consumptions with a low potential loss, the highest nitrogen mass recovery and a partially inhibited methanogenesis. To conclude, is important to remember that this system does three different processes at once with only one energetic consumption, which means, for example, that it is possible to remove 1.25 Nm<sup>3</sup> of CO<sub>2</sub>, 2 kg of COD and recover 0.33 kg of nitrogen with only 1 kWh.

### Declaration of competing interest

The authors declare that they have no known competing financial interests or personal relationships that could have appeared to influence the work reported in this paper.

### Data availability

Data will be made available on request.

### Acknowledgments

Prof. Mauro Majone is acknowledged for his skillful assistance during each step of this experimentation.

### References

- W. Zappa, M. Junginger, M. van den Broek, Is a 100% renewable European power system feasible by 2050? *Appl. Energy* 233–234 (2019) 1027–1050, <https://doi.org/10.1016/j.apenergy.2018.08.109>.
- J.A. Martens, A. Bogaerts, N. De Kimphe, P.A. Jacobs, G.B. Marin, K. Rabaey, M. Saeys, S. Verhelst, The chemical route to a carbon dioxide neutral world, *ChemSusChem* 10 (2017) 1039–1055, <https://doi.org/10.1002/cssc.201601051>.
- A. Mattioli, G.B. Gatti, G.P. Mattuzzi, F. Cecchi, D. Bolzonella, Co-digestion of the organic fraction of municipal solid waste and sludge improves the energy balance of wastewater treatment plants: Rovereto case study, *Renew. Energy* 113 (2017) 980–988, <https://doi.org/10.1016/j.renene.2017.06.079>.
- I. Angelidaki, L. Treu, P. Tsapekos, G. Luo, S. Campanaro, H. Wenzel, P.G. Kougias, Biogas upgrading and utilization: current status and perspectives, *Biotechnol. Adv.* 36 (2018) 452–466, <https://doi.org/10.1016/j.biotechadv.2018.01.011>.
- P. Battle-Vilanova, L. Rovira-Alsina, S. Puig, M.D. Balaguer, P. Icaran, V. M. Monsalvo, F. Rogalla, J. Colprim, Biogas upgrading, CO<sub>2</sub> valorisation and economic reevaluation of bioelectrochemical systems through anodic chlorine production in the framework of wastewater treatment plants, *Sci. Total Environ.* 690 (2019) 352–360, <https://doi.org/10.1016/j.scitotenv.2019.06.361>.
- E. Ryckebosch, M. Drouillon, H. Vervaeren, Techniques for transformation of biogas to biomethane, *Biomass Bioenergy* 35 (2011) 1633–1645, <https://doi.org/10.1016/j.biombioe.2011.02.033>.
- F. Bauer, T. Persson, C. Hultheberg, D. Tamm, Biogas upgrading - technology overview, comparison and perspectives for the future, *Biofuels, Bioprod. Biorefining.* 7 (2013) 499–511, <https://doi.org/10.1002/bbb.1423>.
- R. Kapoor, P. Ghosh, M. Kumar, V.K. Vijay, Evaluation of biogas upgrading technologies and future perspectives: a review, *Environ. Sci. Pollut. Res.* (2019), <https://doi.org/10.1007/s11356-019-04767-1>.
- S.N.B. Villadsen, P.L. Fosbol, I. Angelidaki, J.M. Woodley, L.P. Nielsen, P. Møller, The potential of biogas: the solution to energy storage, *ChemSusChem* 12 (2019) 2147–2153, <https://doi.org/10.1002/cssc.201900100>.
- A. Trzcinski, D. Stuckey, Microbial biomethane production from solid wastes: technologies and applications, <https://doi.org/10.1201/9781351246101-5>, 2017.
- N. Scarlat, J.F. Dallemand, F. Fahl, Biogas: developments and perspectives in Europe, *Renew. Energy* 129 (2018) 457–472, <https://doi.org/10.1016/j.renene.2018.03.006>.
- L. Soussan, J. Riess, B. Erable, M.L. Delia, A. Bergel, Electrochemical reduction of CO<sub>2</sub> catalysed by *Geobacter sulfurreducens* grown on polarized stainless steel cathodes, *Electrochem. Commun.* 28 (2013) 27–30, <https://doi.org/10.1016/j.elecom.2012.11.033>.
- E. Blanchet, Z. Vahlas, L. Etcheverry, Y. Rafrafi, B. Erable, M.L. Delia, A. Bergel, Coupled iron-microbial catalysis for CO<sub>2</sub> hydrogenation with multispecies microbial communities, *Chem. Eng. J.* 346 (2018) 307–316, <https://doi.org/10.1016/j.cej.2018.03.191>.
- M. Villano, F. Aulenta, C. Ciucci, T. Ferri, A. Giuliano, M. Majone, Bioelectrochemical reduction of CO<sub>2</sub> to CH<sub>4</sub> via direct and indirect extracellular electron transfer by a hydrogenophilic methanogenic culture, *Bioresour. Technol.* 101 (2010) 3085–3090, <https://doi.org/10.1016/j.biortech.2009.12.077>.
- M. Rosenbaum, F. Aulenta, M. Villano, L.T. Angenent, Cathodes as electron donors for microbial metabolism: which extracellular electron transfer mechanisms are involved? *Bioresour. Technol.* 102 (2011) 324–333, <https://doi.org/10.1016/j.biortech.2010.07.008>.
- M.C.A.A. van Eerten-Jansen, N.C. Jansen, C.M. Plugge, V. de Wilde, C.J. N. Buisman, A. ter Heijne, Analysis of the mechanisms of bioelectrochemical methane production by mixed cultures, *J. Chem. Technol. Biotechnol.* 90 (2015) 963–970, <https://doi.org/10.1002/jctb.4413>.
- P. Chong, B. Erable, A. Bergel, Microbial anodes: what actually occurs inside pores? *Int. J. Hydrogen Energy* 44 (2019) 4484–4495, <https://doi.org/10.1016/j.ijhydene.2018.09.075>.
- M. Oliot, P. Chong, B. Erable, A. Bergel, Influence of the electrode size on microbial anode performance, *Chem. Eng. J.* 327 (2017) 218–227, <https://doi.org/10.1016/j.cej.2017.06.044>.
- E. Roubaud, R. Lacroix, S. Da Silva, J. Esvan, L. Etcheverry, A. Bergel, R. Basséguy, B. Erable, Industrially scalable surface treatments to enhance the current density output from graphite bioanodes fuelled by real domestic wastewater, *iScience* (2021), 102162, <https://doi.org/10.1016/j.isci.2021.102162>.
- L. Cristiani, J. Ferretti, M. Zeppilli, Electrons recycle concept in a microbial electrolysis cell for biogas upgrading, *Chem. Eng. Technol.* (2021), <https://doi.org/10.1002/ceat.202100534>.
- U. Schröder, F. Harnisch, L.T. Angenent, Microbial electrochemistry and technology: terminology and classification, *Energy Environ. Sci.* 8 (2015) 513–519, <https://doi.org/10.1039/c4ee03359k>.
- M. Zeppilli, E. Dell'Armi, L. Cristiani, M.P. Papini, M. Majone, Reductive/oxidative sequential bioelectrochemical process for perchloroethylene removal, *Water (Switzerland)* (2019) 11, <https://doi.org/10.3390/w11122579>.
- M. Zeppilli, B. Matturro, E. Dell'Armi, L. Cristiani, M.P. Papini, S. Rossetti, M. Majone, Reductive/oxidative sequential bioelectrochemical process for Perchloroethylene (PCE) removal: effect of the applied reductive potential and microbial community characterization, *J. Environ. Chem. Eng.* 9 (2021), 104657, <https://doi.org/10.1016/j.jece.2020.104657>.
- R. Kakarla, B. Min, Sustainable electricity generation and ammonium removal by microbial fuel cell with a microalgae assisted cathode at various environmental conditions, *Bioresour. Technol.* 284 (2019) 161–167, <https://doi.org/10.1016/j.biortech.2019.03.111>.
- P. Kuntke, T.H.J.A. Sleutels, M. Saakes, C.J.N. Buisman, Hydrogen production and ammonium recovery from urine by a Microbial Electrolysis Cell, *Int. J. Hydrogen Energy* (2014), <https://doi.org/10.1016/j.ijhydene.2013.10.089>.
- Y. Ye, H.H. Ngo, W. Guo, Y. Liu, S.W. Chang, D.D. Nguyen, J. Ren, Y. Liu, X. Zhang, Feasibility study on a double chamber microbial fuel cell for nutrient recovery from municipal wastewater, *Chem. Eng. J.* 358 (2019) 236–242, <https://doi.org/10.1016/j.cej.2018.09.215>.
- M. Zeppilli, L. Cristiani, E. Dell'Armi, M. Villano, Potentiostatic vs galvanostatic operation of a Microbial Electrolysis Cell for ammonium recovery and biogas upgrading, *Biochem. Eng. J.* 167 (2021), 107886, <https://doi.org/10.1016/j.bej.2020.107886>.
- M. Zeppilli, L. Cristiani, M. Majone, Bioelectromethanogenesis reaction in a tubular Microbial Electrolysis Cell (MEC) for biogas upgrading, *Renew. Energy* 158 (2019) 23–31, <https://doi.org/10.1016/j.renene.2020.05.122>.
- H. Beyenal, SYSTEMS BIOFILMS IN from Laboratory Practice to Data, (n.d.).
- M. Zeppilli, L. Cristiani, M. Villano, M. Majone, Carbon Dioxide Abatement and Biofilm Growth in MEC equipped with a packed bed adsorption column, *Chem. Eng. Trans.* 86 (2021) 421–426, <https://doi.org/10.3303/CET2186071>.
- R.C. Wagner, J.M. Regan, S.E. Oh, Y. Zuo, B.E. Logan, Hydrogen and methane production from swine wastewater using microbial electrolysis cells, *Water Res.* 43 (2009) 1480–1488, <https://doi.org/10.1016/j.watres.2008.12.037>.
- L. Cristiani, M. Zeppilli, M. Villano, M. Majone, Role of the organic loading rate and the electrodes' potential control strategy on the performance of a micro pilot tubular microbial electrolysis cell for biogas upgrading, *Chem. Eng. J.* 426 (2021), 131909, <https://doi.org/10.1016/j.cej.2021.131909>.
- M. Zeppilli, P. Paiano, C. Torres, D. Pant, A critical evaluation of the pH split and associated effects in bioelectrochemical processes, *Chem. Eng. J.* 422 (2021), 130155, <https://doi.org/10.1016/j.cej.2021.130155>.
- L. Cristiani, M. Zeppilli, C. Porcu, M. Majone, Ammonium recovery and biogas upgrading in a tubular micro-pilot microbial electrolysis, <https://doi.org/10.3390/molecules25122723>, 2020.
- M. Zeppilli, D. Pavesi, M. Gottardo, F. Micolucci, M. Villano, M. Majone, Using effluents from two-phase anaerobic digestion to feed a methane-producing microbial electrolysis, *Chem. Eng. J.* 328 (2017) 428–433, <https://doi.org/10.1016/j.cej.2017.07.057>.
- M. Zeppilli, A. Mattia, M. Villano, M. Majone, Three-chamber bioelectrochemical system for biogas upgrading and nutrient recovery, *Fuel Cell.* 17 (2017) 593–600, <https://doi.org/10.1002/fuce.201700048>.
- T.H.J.A. Sleutels, H.V.M. Hamelers, R.A. Rozendal, C.J.N. Buisman, Ion transport resistance in Microbial Electrolysis Cells with anion and cation exchange membranes, *Int. J. Hydrogen Energy* 34 (2009) 3612–3620, <https://doi.org/10.1016/j.ijhydene.2009.03.004>.
- E. Roubaud, R. Lacroix, S. Da Silva, A. Bergel, R. Basséguy, B. Erable, Catalysis of the hydrogen evolution reaction by hydrogen carbonate to decrease the voltage of microbial electrolysis cell fed with domestic wastewater, *Electrochim. Acta* 275 (2018) 32–39, <https://doi.org/10.1016/j.electacta.2018.04.135>.